Scalable Non-injection Synthesis of Cd-Free Copper Indium Sulfide/Zinc Sulfide Quantum Dots for Third-Gen Photovoltaic Application

Yaxin Zheng, Bahareh Sadeghimakki, Navid. M. S. Jahed, and Siva Sivoththaman
Center for Advanced Photovoltaics and Display Systems, Electrical & Computer Engineering Department, University of Waterloo, 200 University Ave. West, Waterloo, ON N2L 3G1, Canada

ABSTRACT

Copper Indium Sulfide (CIS)-based quantum dots (QDs) are considered as a safer alternative compared to carcinogenic cadmium- and lead-based QDs. Here, we present a facile, high throughput, and non-injection method of synthesizing CIS-based QDs. The structure, shape, size, and crystalline structure of the synthesized QDs were studied using high resolution transmission electron microscopy (HRTEM). The effects of temperature and compositional dependency on the structure and optical properties of the resulting QDs were investigated using elemental, absorption, photoluminescence (PL), and time-resolved spectroscopic analyses. We observed that a gradient increase of temperature during the core growth, as well as addition of excess indium (In) and zinc (Zn) precursors during core and core/shell synthesis, at low growth temperatures, resulted in QDs with improved PL and lifetime. The large Stokes shift, broad emission spectra, and long-lived emission of the synthesized QDs reveal their potential applicability to third generation photovoltaic and optoelectronic devices.

INTRODUCTION

I-III-VI quantum dots (QDs), including copper indium sulfide (CuInS$_2$) (CIS), CuInSe$_2$ (CISe), AgInS$_2$ (AIS), and AgInSe$_2$ (AISe) [1], have attracted considerable attention due to their tunable opto-electrical properties, low bandgap (1.45 eV) [2], lower toxicity [3], and diverse applicability in fields ranging from bioimaging to photovoltaic and opto-electronic devices [4, 5]. High throughput synthesis of CIS QDs has previously been reported [1]. Also, it has been shown that employing different molar ratios of I, III, and VI group elements allow control over the structure and optical properties of the resulting QDs [6]. Herein, we describe the synthesis of CIS QDs with gram-scale throughput at much lower reaction temperatures using two different temperature ramping profiles. As the produced QDs represents a new group of QDs synthesized at a lower temperature regime, the effects of compositional and temperature dependence on their structural and excitonic luminescence were examined. The obtained properties are attractive for photovoltaic and light-emitting devices.

EXPERIMENT

CIS colloidal quantum dots were synthesized based on a previously developed non-injection method [1], with modifications to allow synthesis at lower reaction temperatures. The QD synthesis is carried out in a three-neck flask under an oxygen- and moisture-free atmosphere using Schlenk line technique. A stirring heating mantle is used to heat the reaction chamber and stir the solution. A condenser is connected to the set-up to condensate and return the evaporated fumes of precursor materials into the reaction flask. A cold trap captures and densifies fumes before they are able to reach the vacuum line connected to exhaust.

Materials including indium acetate (99.99%), copper iodide (99.999%), 1-dodecanethiol (DDT, >98%), sulfur (99.98%), 1-Octadecene (ODE, >95%), trioctylphosphine (TOP, 97%), HPLC hexane, chloroform, ethanol, and acetone were purchased from Sigma-Aldrich. Zinc stearate was purchased from Fisher Scientific.

Synthesis route for the growth of core CIS QDs

0.292 g (1 mmol) of indium acetate, 0.19 g (1 mmol) of copper iodide, and 5 ml of 1-dodecanethiol (DDT) are added to a three-neck flask. Different molar ratios of Cu:In were also examined. The reaction flask is sealed and degassed under 20 psi vacuum for 15 minutes, then purged with nitrogen for 20 cycles. The chamber is kept at 80°C for approximately 20 minutes until the precursor mixture becomes a transparent, nearly clear fluid. In the abrupt temperature ramping method, the temperature is increased to 180°C immediately following the 80°C growth period. In the gradient temperature ramp approach, the temperature is gradually raised from 120ºC to 140ºC in 10ºC increments, with 15-20 min waiting time between each ramp. The growth of QDs starts upon decomposition of the solid precursors in DDT. Over time, the solution undergoes a color change from green to yellow, orange, red, dark red and then black. This is indicative of colloidal nanocrystal growth and can be correlated to increasing nanoparticles' size. Upon reaching the desired colour, the reaction is quenched by briefly immersing the reaction flask in a cool water bath. The solution is dispersed in chloroform, hexane or toluene, and subjected to several cycles of washing. QDs are extracted by precipitating with the addition of acetone or ethanol, and centrifuging the mixture. The supernatant is subsequently removed, and the precipitate is dispersed in an organic solvent. This process produces DDT-ligated CIS QDs in grams-scale (up to 0.7 g), making it suitable for scalable large area PV applications.

Synthesis route for the growth of core/shell CIS/ZnS QDs

After thorough washing and redispersing in an organic solvent, 1 ml of CIS QDs are placed in a reaction flask with 4 ml of 1-octadecene. The reaction flask is degassed and purged with nitrogen via the process described in the previous section. To prepare the precursor solution for ZnS overcoating, 0.4 mmol zinc acetate and 0.4 mmol sulfur are dissolved in 5 ml TOP and 4 ml ODE, in a clean glass vial. Different molar ratios of Zn:S were also examined. The overcoat solution is sonicated for 90 minutes, until all precursors are dissolved and the solution becomes uniform. The temperature of the reaction flask is gradually raised up to 160°C, and the overcoat solution is added dropwise to the core solution over the course of 10 minutes, until desired color is reached. The process can be halted by immersing the reaction flask in water bath, or fast extraction using a syringe. The trioctylphosphine oxide (TOPO) ligated core/shell CIS/ZnS QDs are subsequently washed and redispersed in organic solvent, as described above.

DISCUSSION

Structural, elemental, and optical analyses were performed on the synthesized QDs using High Resolution Transmission Electron Microscopy (HRTEM), Energy-Dispersive X-Ray Spectroscopy (EDS), Inductively Coupled Plasma Mass Spectrometry (ICP-MS), UV-vis absorption, PL, and time-resolved spectroscopy. The effects of compositional ratio and temperature ramping profile variation on the properties of QDs were investigated.

Structural and elemental analyses of CIS core and CIS/ZnS core/shell QDs

The TEM images shown in Figure 1.a , 1.b. and their diffraction patterns (bottom insets) demonstrate the spherical shape and polydispersity of the synthesized core CIS and core/shell CIS/ZnS QDs, respectively. The crystal structure of the QDs, spherical shape, as well as their sizes (4 nm for core and 2.5 nm for core/shell) are apparent from the HRTEM images (top insets). The elemental composition for the core CIS (Cu, In, S) and core/shell CIS/ZnS (Cu, In, S, Zn) QDs were detected using EDS analysis (see Figure 1.c). Using elemental mapping, corresponding compositions were also detected on the CIS/ZnS, as shown in Figure 1.d. ICP-MS spectroscopy was performed for the CIS core QDs synthesized with a Cu:In molar ratio of 1:2, grown using two different temperature ramping profiles. The results shown in Figure 1.e suggest non-stoichiometric Cu:In:S ratios of 1:2:0.25 and 1:3:0.4 for QDs grown using gradient and abrupt temperature schemes, respectively.
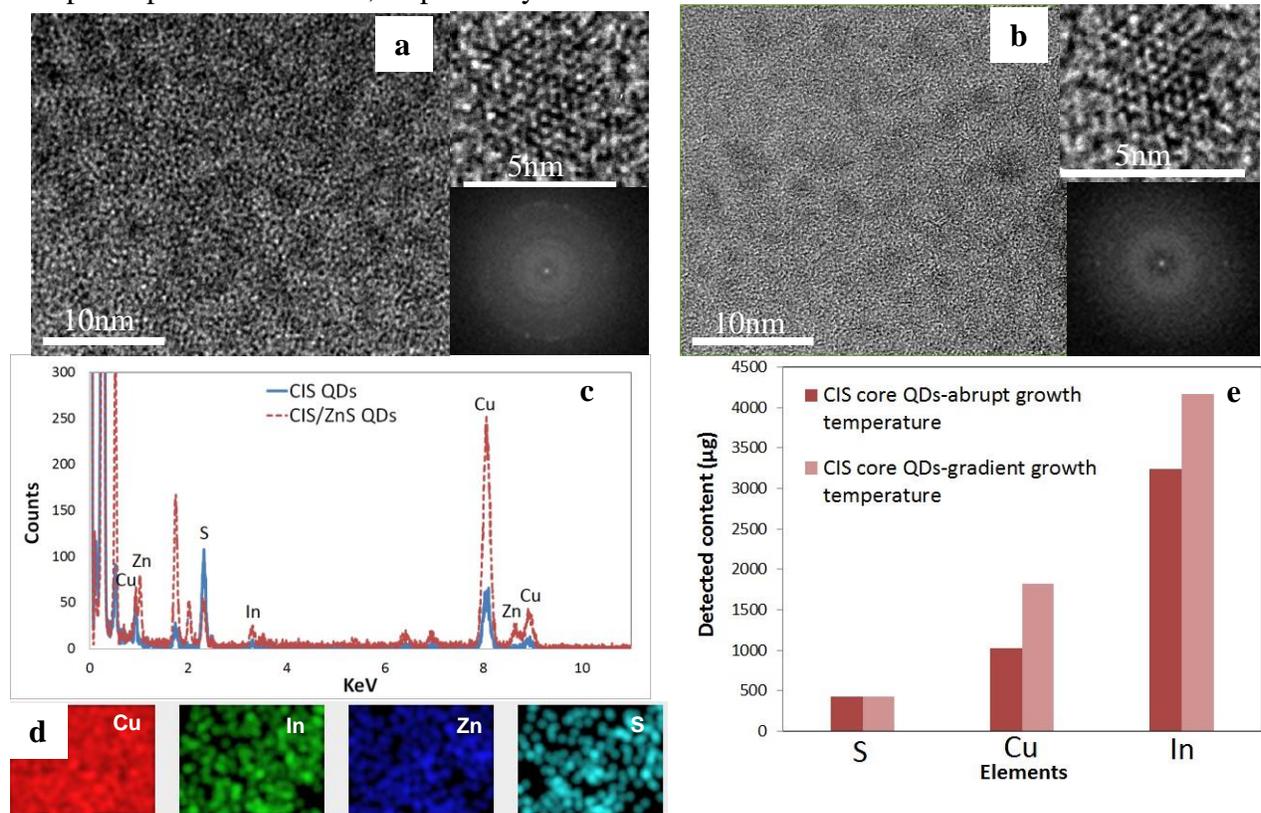

Figure 1.TEM, diffraction patterns and HRTEM (insets) images of a) core CIS and b) core/shell CIS/ZnS QDs, c) EDS analyses on CIS and CIS/ZnS QDs, d) elemental mapping on CIS/ZnS QDs, e) ICP-MS analyses on CIS QDs synthesized with abrupt and gradient temperature ramps .

Optical analysis of CIS and CIS/ZnS core/shell QDs

Figure 2.a shows the emission spectra of core CIS QDs synthesized with Cu:In molar ratios of 1:1, extracted at different growth times. The measurements indicate broad emission spectra ranging from visible to near infrared. The shoulder that appears in the emission peaks matches with observations reported in literature [7], and can be attributed to the inhomogeneity of the QDs and defect sites resulting from their small size.

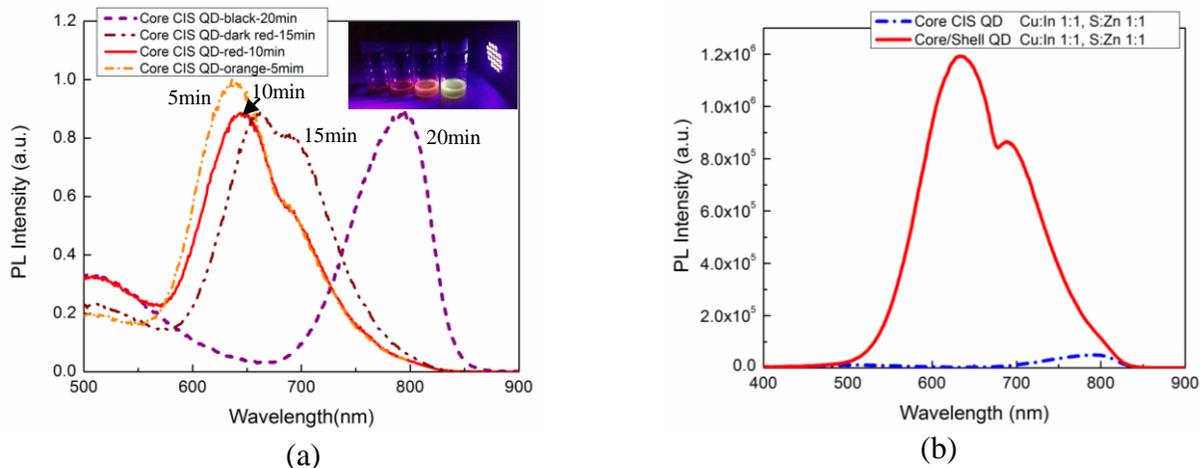(a)   (b)

Figure 2. a) Emission spectra of CIS QDs extracted at different growth times. Inset shows the QDs illuminated by UV-lamp. b) PL spectra of CIS core and CIS/ZnS core/shell QDs. The molar ratios used are Cu:In 1:1, Zn:S 1:1.

Figure 2.b. shows the 10-fold increase in PL intensity and up to 160 nm peak position shift obtained after 20 min shell growth on the CIS core using overcoat with Zn:S molar ratio of 1:1. This result indicates that through shell growth, an even higher degree of tunability in QD size and emission wavelength can be achieved. The observed luminescence blue shift could be attributed to the exchange of CIS cations with zinc, resulting in shrinking of the QD core size [8], potential surface reconstruction [3], and inter-diffusion of Zn atoms into the core [2].

Compositional dependence on excitonic luminescence in CIS-based QDs

The effects of Cu:In molar ratio variation on the properties of the synthesized core structures were examined. As shown in Figure 3.a., it was observed that, in close agreement with literature [6], copper deficiency produced with 1 mmol:2 mmol Cu:In resulted in core QDs with the highest PL. The results also showed that, at a fixed growth time and using different Cu:In ratios, different sizes of QDs were obtained. This observation demonstrates that the bandgaps of the QDs are tunable via varying the composition of the reactants.

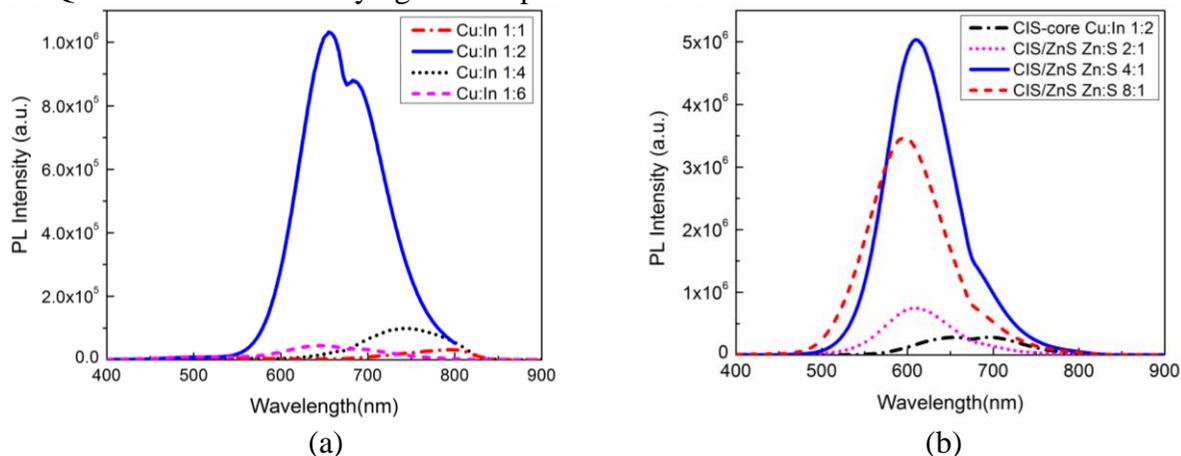(a)   (b)

Figure 3. a) CIS QD obtained using different Cu:In molar ratios, b) CIS/ZnS QDs obtained using different Zn:S molar ratios.

Different composition ratios of Zn:S were also used for shell growth. As shown in Figure 3.b, the PL intensity of the core/shell QDs improved by increasing Zn:S molar ratio. Excess zinc allows inter-diffusion of Zn atoms to the core, resulting in filling of copper vacancies and removal of interstitial atoms produced during cation exchange [8]. This reaction produces ZCIS/ZnS or CIS/Zn-CIS/ZnS structures [6] with a higher degree of passivation. Further investigation is required to confirm vacancy filling by inter-diffused Zn. The result also indicates that only the 650 nm emission peak of the core structure is blue-shifted after shell growth. The second peak, at 720 nm, does not blue-shift, becoming a weak shoulder instead. The 720 nm emission can be attributed to the inhomogeneity of QDs and defect sites, which is removed by Zn passivation [7].

Figure 4 demonstrates the improvement of decay lifetime of the CIS/ZnS QDs when the Zn:S molar ratio is increased. Table 1 presents lifetime components in the range of tens to hundreds of nanoseconds, extracted from multi-exponential tail fitting analyses for the core and the core/shell QDs, respectively. The measurements are indicative of QDs with long-lived emission. Lifetime was increased from 84.33 ns for the CIS core QDs, to 157.99 ns for the CIS/ZnS core/shell QDs when overcoating with a Zn:S molar ratio of 8:1.
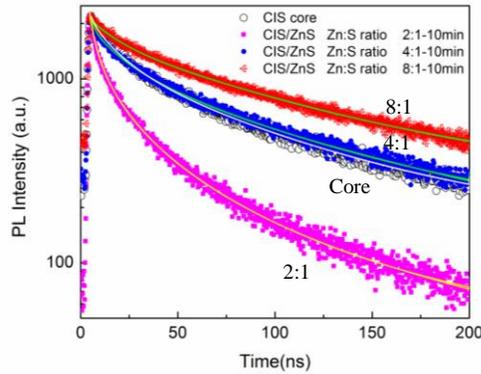

Figure 4. Evolution of decay lifetime of CIS/ZnS QDs using excess Zn. Solid lines are the best fit

Table 1. Decay lifetime components for core CIS and core/shell CIS/ZnS QDs obtained from multi-exponential fitting analyses

Sample	B_1	τ_1 (ns)	B_2	τ_2 (ns)	B_3	τ_3 (ns)	χ^2
CIS	207.80	2.857	780.29	16.419	1050.6	84.33	1.016
CIS/ZnS Zn:S 2:1	853.99	2.814	690.43	11.394	212.35	167.91	1.078
CIS/ZnS Zn:S 4:1	328.36	1.757	353.12	10.976	829.60	103.54	1.066
CIS/ZnS Zn:S 8:1			498.58	15.187	1324.7	157.99	1.031

B: *pre-exponential factor*
τ: *decay lifetime component (ns)*
χ^2: fit quality indicator (*assured by criteria χ2 <1.3*)

Temperature dependence on excitonic luminescence in CIS-based QDs

To further improve core quality, CIS QDs were synthesized using gradual and abrupt increases in reaction temperature (as described above); their properties were examined and compared. The PL of the core QDs grown using gradient temperature ramp showed a 10-fold improvement from the PL of the core QDs produced by abrupt temperature ramp (see Figure 5.a). Large Stokes shifts of 230 nm and 140 nm can be seen for the QDs grown using gradient and abrupt temperature ramps, respectively. Core CIS QDs with photoluminescence quantum yield (PLQY) of 7% and improved lifetime were obtained using the gradient temperature ramp.

Core/shell QDs were synthesized from the CIS core grown using the gradient temperature ramping method. The overcoating was performed at different growth temperatures ranging from 70 ℃ to 160℃, using a Zn:S molar ratio of 8:1. The PL and lifetime of the obtained core/shell structures improved with increase in reaction temperature. Core/shell CIS/ZnS QDs with PLQY of 20% was obtained at a maximum temperature of 160℃. Figure 5.b

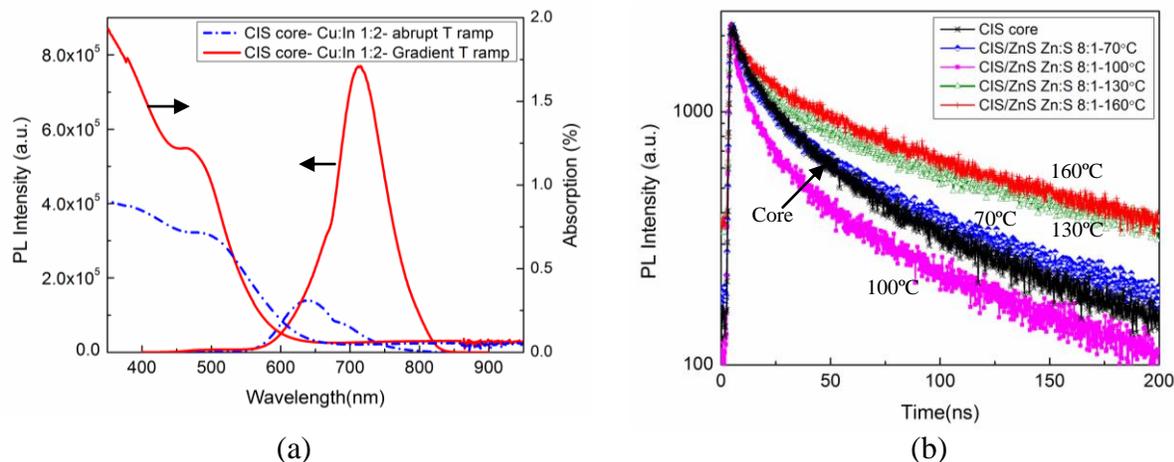|	
(a)	(b)

Figure 5. a) Absorption and PL of CIS QDs synthesized using abrupt and gradient temperature ramps, b) lifetime of the CIS/ZnS QDs produced at different shell growth temperatures.

demonstrates the evolution of the lifetime of CIS/ZnS QDs extracted after 10 min of overcoating and grown at increasingly higher temperatures.

CONCLUSIONS

CIS core and CIS/ZnS core/shell QDs with high throughput and intense PL were successfully synthesized using a non-injection method. Different molar ratios of Cu:In and Zn:S were employed to control the structure and optical properties of the resultant QDs. It was observed that using an excess of In and Zn components during core and core/shell synthesis, respectively, resulted in QDs with improved PL and lifetime. The results also demonstrate that the bandgap of the QDs is tunable via control over QD size and reactant composition. A PLQY of 7% was achieved for CIS core QDs grown with gradient temperature ramp, at a maximum temperature of 140°C. Core/shell CIS/ZnS QDs with PLQY of 20% was obtained at 160ºC from this core QDs. The long-lived emission (85 ns-158 ns) of the obtained CIS-based QDs is a critical parameter for improving transport properties for application in semiconductor devices.

REFERENCES

1. L. Li, A. Pandey, D. J. Werder, B. P. Khanal, J. M. Pietryga, and V. I. Klimov, J. Am. Chem. Soc., **133**, 1176 (2011).
2. T. Pons, E. Pic, N. Lequeux, E. Cassette, L. Bezdetnaya, F. Guillemin, F. Marchal and B. Dubertret, ACS Nano, **4**, 2531 (2010).
3. L. Li, T. J. Daou, I. Texier, T. K. C. Tran, Q. L. Nguyen, P. Reiss., Chem Mater, **21**, 2422 (2009).
4. J. M. Bruchez, M. Moronne, P. Gin, S. Weiss, A. P. Alivisatos, Science, **281**, 2013 (1998).
5. C. Steinhagen, M. G Panthani, V. Akhavan, B. Goodfellow, B. Koo, B.A. Kogel., J. Am. Chem. Soc., **131**, 12554 (2009).
6. M. Fu, W. Luan, S.T. Tu, and L. Mleczko, J. Nanomater, **2015**, 1(2015).
7. L. De Trizio, M. Prato, A. Genovese, A. Casu, M. Povia, R. Simonutti, M. J. P. Alcocer, C. D'Andrea, F. Tassone and L. Manna, Chem. Mater., **24**, 2400 (2012).
8. J. Park and S.W. Kim, J. Mater. Chem., **21**, 3745 (2011)